

Reversed cyclic response of reinforced concrete bridge piles in cohesionless soil

Hutchinson, T.C.¹ and Chai, Y.H.²

ABSTRACT

In seismic design of bridges, many situations arise where the predominant inelastic deformation of the bridge system occurs within the pile-supported foundation. In such cases, the overall performance of the bridge structure depends on the local ductility capacity of the supporting piles as well as the strength and stiffness of the surrounding soil.

A research program was initiated at the University of California, Davis to investigate the plastic hinging of reinforced concrete piles in cohesionless soil. Full-scale test piles with reinforcement details representative of the California Department of Transportation (Caltrans) current design for 70-ton piles were tested under combined axial compression and quasi-static reversed cyclic lateral load. The piles were tested with above-ground heights of $2D$ and $6D$ and in loose and dense (dry) sand conditions. Results from the four pile tests are presented in this paper with an emphasis on the characterization of the local deformation of the piles below ground.

INTRODUCTION

In seismic design of bridges, it is generally accepted that the foundation system will be provided with a lateral strength larger than that of the superstructure, thereby ensuring that the predominant inelastic deformation occurs above ground. This allows for ease of post-earthquake inspection and repair if necessary. However, many design situations arise where plastic hinging will occur within the pile shafts below ground. A good example of such design is the multi-column bent where the columns are extended below ground as pile-shafts of the same diameter. Such substructure design is cost-effective when compared to the column/pile-cap/pile combination since the construction of an expensive pile-cap can be eliminated. Under seismic loading, however, the maximum bending moment in the pile-shaft occurs at some distance below the ground level depending on the relative stiffness of the pile and the surrounding soil. The magnitude of the bending moment under the design level earthquake can be sufficiently large to cause plastic hinging in the piles.

In addition to the difficulty of damage inspection after an earthquake, extensive yielding of the pile below ground level might result in an unacceptable level of residual displacement which would tend to render the structure unserviceable after the earthquake. The design lateral strength of these structures is currently prescribed at higher levels than that of an equivalent column. This is intended to ensure that the full ductility capacity of the piles will not be developed under the design level earthquake even though full detailing requirements are imposed on the design of these members. Such structures have been termed as *Limited Ductility Structures* by ATC-32 where a displacement ductility factor of $Z = 3$ has been adopted for design (ATC-32, 1996). Conservative design, similar to that of ATC-32, is currently prescribed by the New Zealand Bridge Code (Park, 1998).

The overall ductility capacity of a bridge structure will depend on the local ductility capacity of its yielding members. The ductility capacity of a bridge structure can be assessed using a non-linear incremental 'push-over' analysis (Priestly et al, 1996). A static lateral load is applied monotonically to the structure until a full plastic mechanism is developed in the structure. For bridge structures where plastic hinging is expected in the piles the overall ductility capacity of the structure depends on the local ductility capacity of the piles. In this case, the local plastic rotational capacity of the pile can be written as:

$$\theta_p = (\phi_u - \phi_y)L_p \quad (1)$$

where ϕ_u , ϕ_y = ultimate and yield curvature, respectively; and L_p = equivalent plastic hinge length. Under the interaction of soil, the bending moment distribution in the pile is more gradual compared to that of a free-standing column since the surrounding soil will spread the zone of plasticity over a longer length and therefore provide a larger ductility capacity to the pile. Furthermore, the lateral restraint provided by the surrounding soil might increase the ultimate compressive strain of the concrete thereby increasing the ultimate curvature that can be tolerated by the pile. Although an analytical study has shown that the equivalent plastic hinge length for piles

¹Research Assistant, University of California, Davis

²Associate Professor, University of California, Davis

varies from one to two pile diameters depending on the soil stiffness and pile above-ground height (Budek et al. 1994 and M.J.N. Priestly et al, 1996), very few soil-pile interaction tests have been carried out to verify such results. In this paper, preliminary results of an experimental study to investigate the plastification of piles under the interaction of soil will be presented.

EXPERIMENTAL STUDY

The experimental program described in this paper consisted of lateral load tests of four full-scale 406 mm diameter concrete piles under two different soil conditions: loose and dense (dry) sand. Above-ground heights of $2D$ and $6D$, where D = diameter of the pile, were used to investigate the influence of the moment gradient on the distribution of pile curvature as well as the associated plastic hinge length.

Test Set-up and Pile Details

Figure 1 shows the reinforcement details and the pertinent parameters for the four test piles. Test pile details were representative of Caltrans current design for 70-ton piles. The test piles were subjected to a combination of axial compression and reversed cyclic quasi-static lateral loading. The lateral loading was imposed by a long-stroke double-acting actuator reacting against a large-capacity concrete reaction block. The axial force applied to the pile was $P = 445$ kN, corresponding to a nominal axial stress level of $0.1 f'_c A_g$.

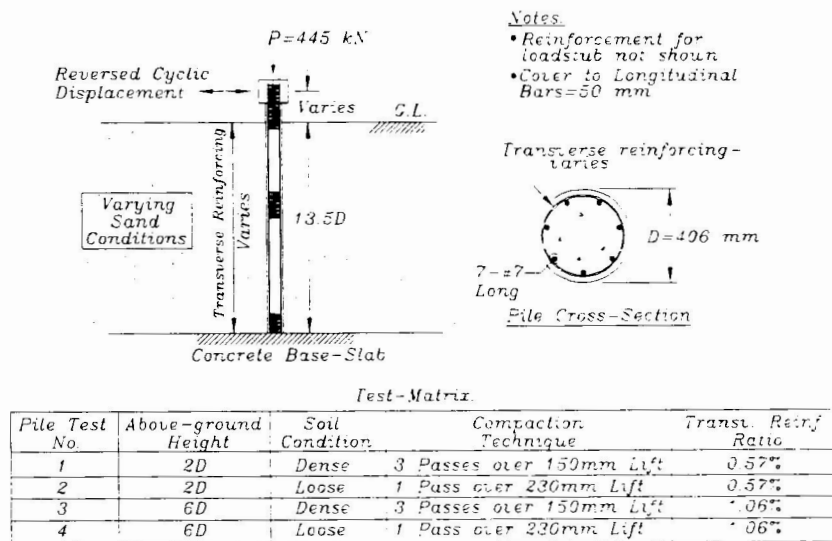


Figure 1: Reinforcement details and test matrix

Soil Properties

A locally available river sand was used as the cohesionless soil for the pile tests. The soil can be classified as clean, poorly graded sand (SP) with about 3% fines (% passing No. 200 sieve) and no gravel (0% retained on No. 4 sieve) in accordance with the Unified Soil Classification System (USCS). To achieve dense sand conditions, the soil was compacted in 150 mm lifts using a 1.8 kN combustion-type vibratory flat-plate compactor with three compaction passes per lift. For loose sand conditions, the soil was compacted in 230 mm lifts using a lighter compactor (1.6 kN). Table 1 summarizes the in-place soil properties as obtained from CPT soundings performed prior to testing. It should be noted that the values listed are the average values within the zone of interest for lateral response (i.e. the upper 1 to 3 m). In order to correct for the influence of overburden pressure on the tip resistance, the tip resistance q_c was normalized to an effective overburden pressure σ'_v of 0.1 MPa using the Liao and Whitman procedure (Liao and Whitman, 1971). The normalized tip resistance is given by $q_{c1} = C_N q_c$ where $C_N = \sqrt{P_a / \sigma'_v}$ with $P_a = 0.1$ MPa and C_N is limited to a maximum value of 2.0.

Pile No.	q_c (MPa)	Friction Ratio, R_f (%)	q_{c1} (MPa)	D_r (%)	Friction Angle, ϕ'	k_o (kN/m ³)
1	14.6	0.45	24.7	85	43	65200
2	3.6	0.17	6.1	54	37	32600
3	10.8	0.33	18.2	79	41	62400
4	4.5	0.35	7.4	56	38	38000

Table 1: Summary of pertinent compacted sand properties (based on CPT soundings)
Note: D_r = relative density and k_o = lateral subgrade modulus

RESULTS

Lateral Force-Displacement Response

Figure 2 shows the measured lateral force versus lateral displacement response of the piles at above ground heights of $2D$ and $6D$ in dense and loose sand conditions. The x-axis corresponds to the lateral displacement at the point of lateral force application, while the y-axis corresponds to the lateral force measured by the horizontal loadcell. Note that the scale for the x and y-axis is different between the piles with different above ground heights. It should also be noted that the lateral force versus lateral displacement response shown in Figure 2 has been corrected for the inclination of the applied axial force and the associated $P - \Delta$ moment. An equivalent elastoplastic yield displacement Δ_y is defined by extrapolating the lateral displacement Δ'_y obtained at the lateral yield force V_y to the maximum lateral force V_{max} i.e.

$$\Delta_y \equiv \Delta'_y \frac{V_{max}}{V_y} \quad (2)$$

The lateral yield force V_y of the soil/pile system was estimated using the first-yield moment of the test pile while taking into account the confinement effect of the transverse reinforcement (Mander et al, 1988) and the resistance of the soil as modelled by non-linear API soil springs (API, 1982).

The hysteretic response of the piles at $2D$ above ground were relatively stable. During the first cycle to the maximum displacement imposed on the system, $\Delta_{max} = 254$ mm, the pile in dense sand showed a lateral strength degradation of 44% (compared to peak lateral force), averaged for the push direction and pull directions. The pile in loose sand, however, exhibited a lesser degradation of strength at approximately 25% (compared to peak lateral force upon displacement to $\Delta_{max} = 351$ mm). It is interesting to note that the maximum lateral forces measured for the piles at $2D$ above ground level, in dense and loose sand conditions were approximately equal even though the tip resistance values from the CPT soundings for the loose sand was about 1/3 that of the dense sand.

The taller, more flexible piles at $6D$ above ground exhibited a significant post-peak strength drop due to the large $P - \Delta$ moment applied on the pile section. For the pile in dense sand, the lateral strength at $\mu_\Delta = 3.7$ was only 12% of the maximum lateral force, while for the pile in loose sand, the lateral strength at $\mu_\Delta = 2.7$ was 26% of the maximum lateral force. The maximum lateral strength of the pile in dense sand was about 15% greater than the pile in loose sand.

For piles at $2D$ above ground level, the displacement ductility capacities, estimated based on a 20% degradation of peak lateral strength and the average value in the two directions of loading, are $\mu_\Delta = 2.6$ for the pile in dense sand and $\mu_\Delta = 3.1$ for the pile in loose sand. The larger ductility capacity for the pile in loose sand can be attributed to the more gradual post-peak degradation of lateral strength when compared to that of the dense sand. For the piles at $6D$ above ground level, the displacement ductility capacities (estimated using the same criteria as for the pile at $2D$ above ground) are $\mu_\Delta = 2.0$ for the pile in dense sand and $\mu_\Delta = 1.8$ for the pile in loose sand.

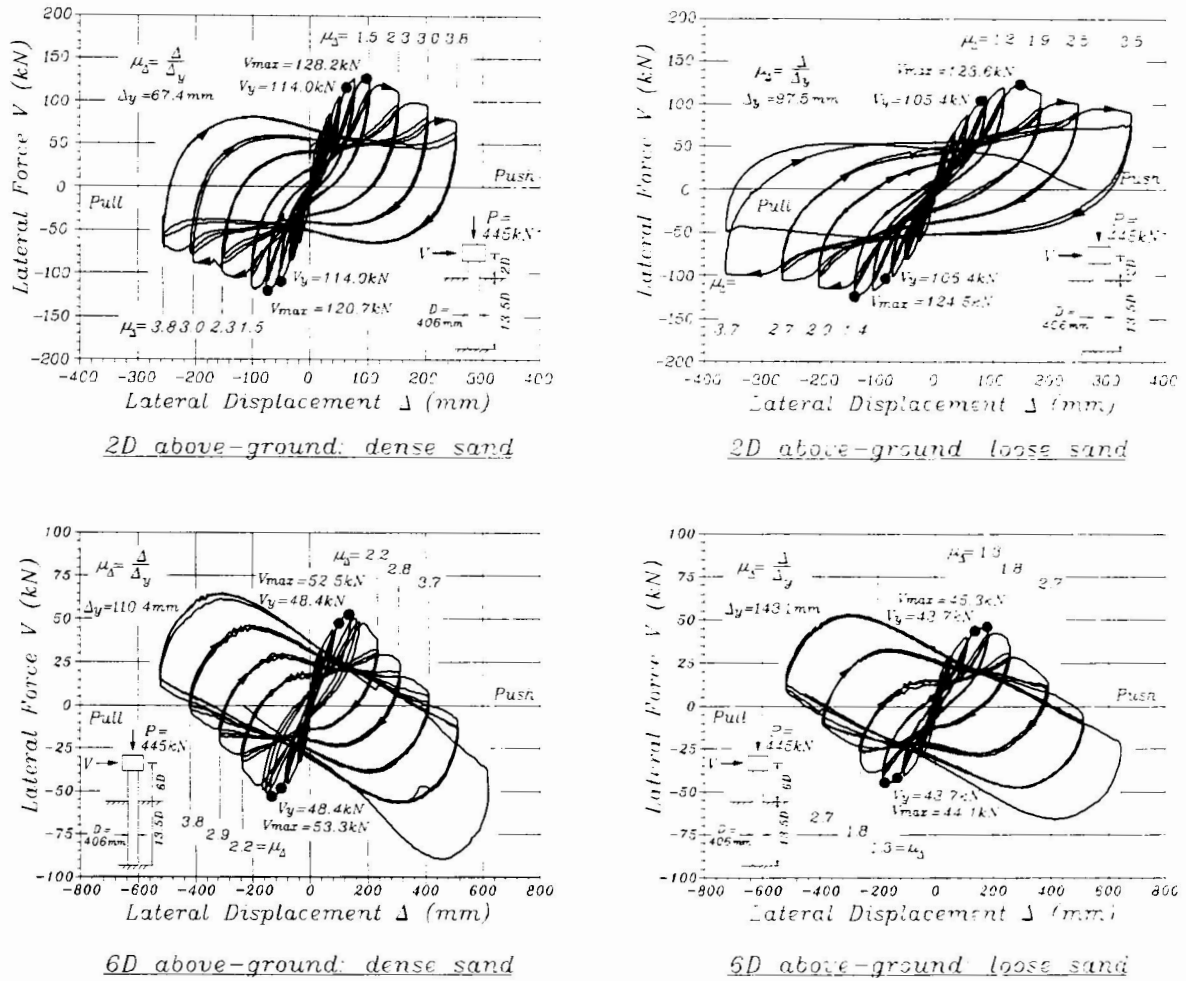


Figure 2: Hysteretic response of soil/pile systems

Curvature Distribution and Observed Pile Damage

Of particular importance in the inelastic behavior of piles is the magnitude of the local deformation upon the formation of the plastic hinge. The local deformation can be characterized in terms of the curvature distribution along the length of the pile. Figure 3 shows the distribution of the measured curvature for the four test piles for displacement ductility factors from $\mu_{\Delta} = \pm 1.1$ to about ± 2.7 . Although the measured curvatures showed a considerable variation, the region of maximum flexural demand was fairly well defined for all of the piles. The equivalent elasto-plastic yield curvature, estimated using a moment-curvature analysis for the confined concrete section, was $\phi_y = 12.98 \times 10^{-3} \text{ rad/m}$ for the piles at 2D above ground level and $\phi_y = 16.96 \times 10^{-3} \text{ rad/m}$ for the piles at 6D above ground level. Using the estimated elasto-plastic yield curvature, the maximum measured curvatures represented a curvature ductility factor $\mu_{\phi} = 11.9$ and 12.9 (at $\mu_{\Delta} = -2.5$ and $\mu_{\Delta} = 2.5$ for the test piles at 2D in dense and loose sand, respectively). For the piles at 6D, the maximum measured curvatures represented a curvature ductility factor $\mu_{\phi} = 6.7$ and 7.3 (at $\mu_{\Delta} = 2.5$ and $\mu_{\Delta} = 2.7$) for the piles in dense and loose sand, respectively. It is worth noting that the measured curvatures, upon integrating with respect to the pile length, were within 18% of the lateral displacement measured at the top of the pile. For displacement ductility factors larger than 2.7, the measured curvature is less reliable due to spalling of the cover concrete which tends to push the cables used for curvature measurement away from the concrete surface.

The measured curvatures allow an equivalent plastic hinge length to be determined. Figure 4 shows the experimentally determined equivalent plastic hinge length, averaged for the two directions of loading and normalized by the pile diameter, versus the displacement ductility factor. For the test piles at 2D above ground level, the

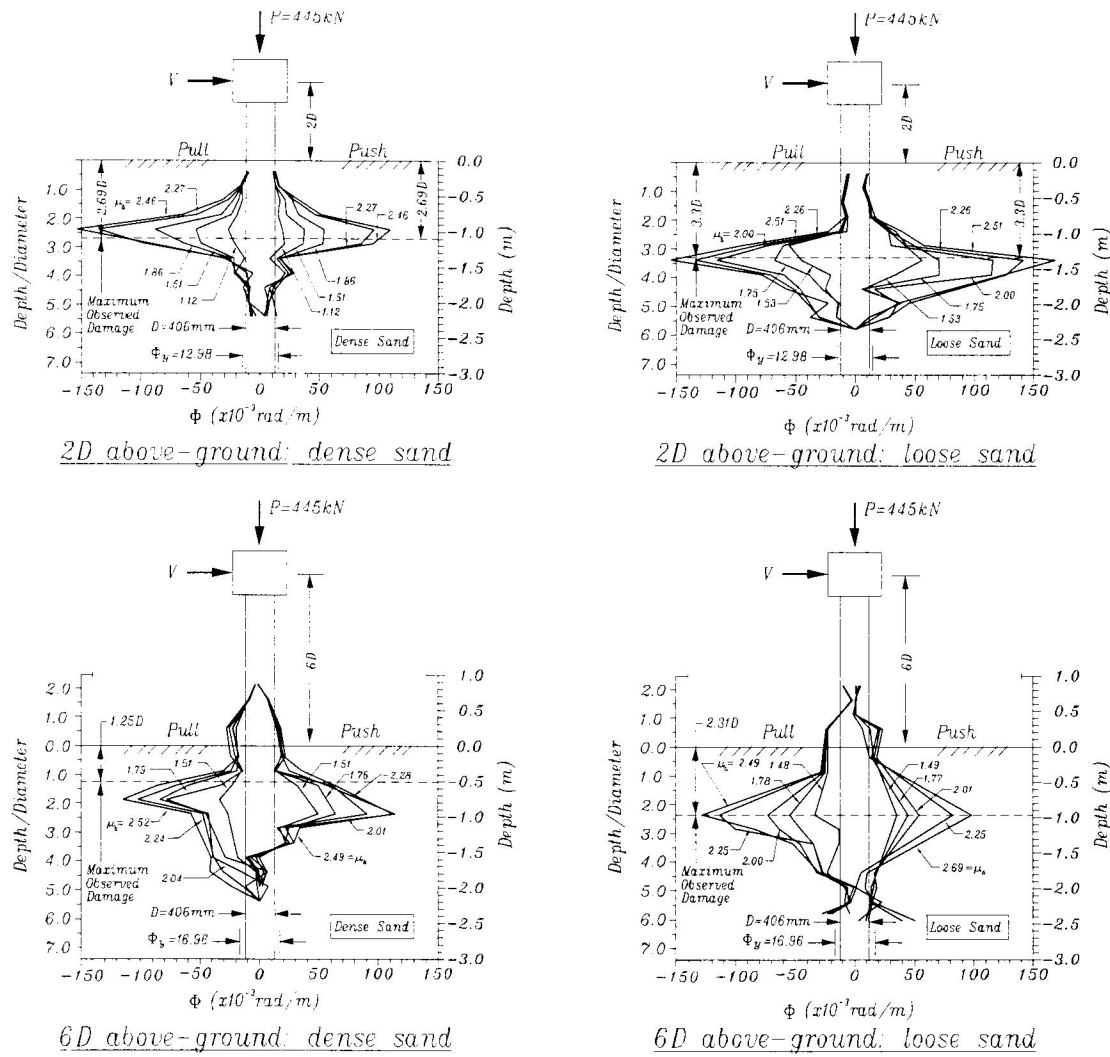


Figure 3: Measured curvature distribution for soil/pile systems

equivalent plastic hinge length is relatively constant with respect to displacement ductility factor and is slightly larger than the pile diameter, with an average of about $1.05D$ for both piles. Note that the equivalent plastic hinge length is slightly larger for the pile in loose sand for $\mu_{\Delta} > 1.75$. For the piles at $6D$ above ground level, the equivalent plastic hinge length is slightly larger, with average values of $1.39D$ and $1.45D$ for the pile in dense and loose sand, respectively.

CONCLUSIONS

This paper presents a preliminary report on a research project to investigate the inelastic behavior of reinforced concrete piles under the interaction of cohesionless soil. Results from piles tested in dense and loose sand with above-ground heights of $2D$ and $6D$ are discussed. For the piles at $2D$ above ground level; in dense sand, the region of maximum bending moment, and hence the largest curvature demand, occurred at a depth of about $2.69D$ below ground level. For the pile in loose sand, the region of maximum moment was about $3.3D$ below ground level. Even though the piles were embedded in soils of different density, the maximum lateral forces were approximately the same for both piles. The experimentally determined equivalent plastic hinge length was about 5% larger than the pile diameter for both piles at $2D$ above ground level and is not sensitive to soil density. The equivalent plastic hinge length was also relatively constant with respect to the displacement ductility factor. At a

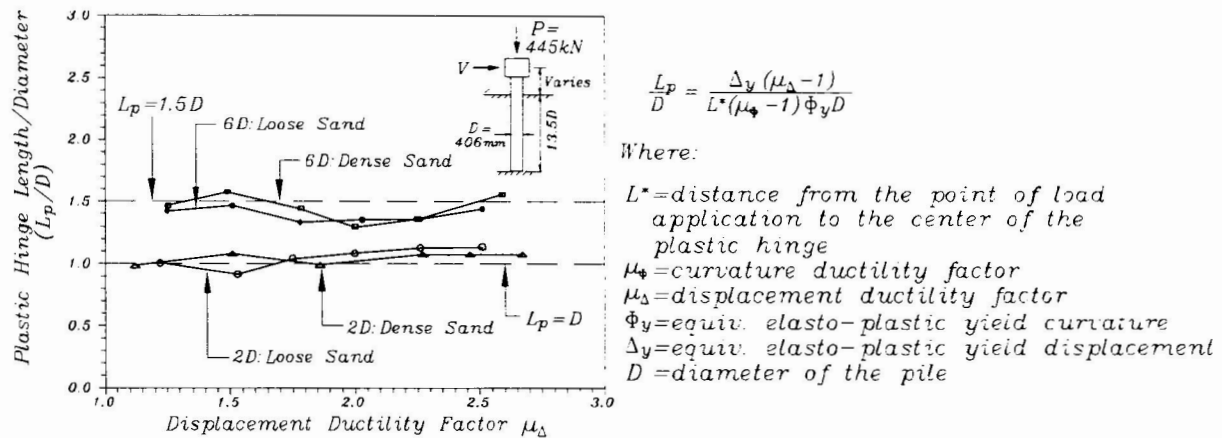


Figure 4: Experimentally determined equivalent plastic hinge length for soil/pile systems

confining steel ratio of $\rho_s = 0.57\%$, test results indicated that the displacement ductility capacity, based on 20% degradation of peak lateral strength, were $\mu_\Delta = 2.6$ and 3.1 for the pile in dense and loose sand respectively.

For the pile at $6D$ above ground level embedded in dense sand, the region of maximum bending moment occurred at a depth of about $1.25D$ below ground level. For the pile in loose sand, the region of maximum moment occurred at about $2.31D$ below ground level. Even though the piles were embedded in soils of different density, the maximum lateral forces were approximately the same for both piles. The experimentally determined equivalent plastic hinge length was about 39% larger than the pile diameter for the pile in dense sand and about 45% larger than the pile diameter for the pile in loose sand. For the piles at $6D$ above ground level, the equivalent plastic hinge length is not sensitive to soil density, and is relatively constant with respect to the displacement ductility factor. The experimentally determined displacement ductility capacity, based on 20% degradation of peak lateral strength, were $\mu_\Delta = 2.0$ and 1.8 for the pile in dense and loose sand, respectively.

ACKNOWLEDGMENTS

The research reported in this paper is funded under Caltrans Research Contract No. 59Y500 where Thomas Sardo is the Contract Monitor and Timothy Leahy is the Contract Manager. The assistance provided by the staffs and students of the Civil Engineering Department at UC Davis, namely, Bill Sluis, Tom Bui, Sam Jamison, Amy Smith, Tom Kohnke, Dennis O'Brien, and the CPT soundings provided by Daniel Speer and Ralph Fitzpatrick of Caltrans are greatly appreciated. The helpful comments of Professor R.W. Boulanger of UC Davis, and Professor M.J.Nigel Priestley and Dr. Andy Budek of UC San Diego are also appreciated.

REFERENCES

- American Petroleum Institute, 1982. Washington, D.C., *API Recommended Practice for Planning, Designing and Constructing Fixed Offshore Platforms*, Thirteenth edition.
- Applied Technology Council, 555 Twin Dolphin Drive, Suite 550. Redwood City, California 94065. *Improved Seismic Design Criteria for California Bridges: Provisional Recommendations*, ATC-32. June 1996.
- Budek, A., Benzoni, G., and Priestley, M.J.N., 1994. *In-ground plastic hinges in column/pileshaft design*. Proceedings of the Third Annual Seismic Research Workshop, Sacramento, California. Caltrans, Department of Transportation, Division of Structures.
- Liao, S.C. and Whitman, R.V., March 1986. *Overburden correction factors for SPT in sand*. Jour. Geotech. Engrg., ASCE, 112(3):373-377.
- Mander, J.B., Priestley, M.J.N., and Park, R., Aug., 1988. *Theoretical stress-strain model for confined concrete*. Jour. Struct. Div., ASCE, 114(8):1804-1826.
- Priestley M.J.N, Seible F., and Calvi G.M., 1996, *Seismic Design and Retrofit of Bridges*. Wiley Interscience, New York.